NeuroToxicology 33 (2012) 902–910

Contents lists available at SciVerse ScienceDirect

NeuroToxicology

The neurotoxic potential of engineered nanomaterials

William K. Boyes [a,*], Rui Chen [b], Chunying Chen [b], Robert A. Yokel [c]

[a] U.S. Environmental Protection Agency, Research Triangle Park, NC, USA
[b] National Center for Nanoscience and Technology, Beijing, China
[c] University of Kentucky, Lexington, KY, USA

ARTICLE INFO

Article history:
Received 11 October 2011
Received in revised form 8 December 2011
Accepted 12 December 2011
Available online 21 December 2011

Keywords:
Biodistribution
Pharmacokinetics
Blood–brain barrier
Cerium oxide (ceria)
Copper
Titanium dioxide (titania)
Phototoxicity

ABSTRACT

The expanding development and production of engineered nanomaterials (ENMs) have diverse and far-reaching potential benefits in consumer products, food, drugs, medical devices and for enhancing environmental cleanup and remediation. The knowledge of potential implications of ENMs, including the potential for inadvertent exposures and adverse neurotoxic consequences, is lagging behind their development. A potential risk for neurotoxicity arises if exposure leads to systemic absorption and distribution to the nervous system. This paper is the summary of a symposium entitled *Neurotoxicity Potential of Engineered Nanomaterials* presented at the 2011 Xi'an International Neurotoxicology Conference held June 5–9 in Xi'an China. The following topics were featured in the symposium: the toxicokinetics of engineered nanomaterials; differential uptake of nanoceria in brain and peripheral organs; translocation into the brain and potential damage following nanoparticle exposure; and the retina as a potential site of nanomaterial phototoxicity. Each of these topics is discussed fully in sections of the manuscript. The promising benefits of ENM technology can be best realized if the potential risks are first understood and then minimized in product and system designs.

Published by Elsevier Inc.

1. Introduction

An industrial revolution is underway involving the development and application of ENMs (National Science and Technology Council, 2007). Their small size (generally defined as having at least one dimension less than 100 nm) can give them unique and desirable properties. For example, ENMs have a high surface area to mass ratio making them more reactive than bulk materials. The unique properties of ENMs have also raised concerns about the potential for unintended consequences on human health and the environment. It is important to study the potential for ENMs to be hazardous prior to their entry into the marketplace or environment.

A key to making such predictions is discovering which features of ENMs could potentially cause adverse consequences for human health or the ecosystem. If these potentially problematic features can be identified early, then material engineers can design products to minimize risk. For neurotoxicity, primary considerations are the extent to which nanomaterials reach the nervous system (including the brain) and the potential mechanisms of neurotoxicity should ENMs access nervous tissue. Answering questions such as these may contribute to safer and more sustainable development of these exciting new technologies. Those developing ENM-enabled drugs might actively seek features that enhance the penetration into tissues such as the brain or the eye, whereas those developing other products and applications would likely try to avoid such properties. In addition, it is important to consider whether any tissue accumulations or adverse outcomes occur under realistic exposure conditions; however there is currently a relative lack of realistic exposure information. Also, the fact that nanomaterial-enabled technologies and applications continue to emerge means that the realistic exposure conditions are presently uncertain.

This synopsis represents a summary of a symposium entitled *Neurotoxicity Potential of Engineered Nanomaterials* that was presented at the Xi'an International Neurotoxicology Conference, Neurotoxicity and Neurodegeneration: Local Effect and Global Impact, held on June 5–10, 2011, in Xi'an, China. The symposium was organized by Drs. William K. Boyes, Syed Ali, and Robert A. Yokel. The speakers in the session included: Dr. Martin Philbert, who presented an overview of nanomaterials in the nervous system, drug applications, benefits, and potential risks; Dr. Robert Yokel, who spoke on the toxicokinetics of ENMs; Drs. Rui Chen and Chunying Chen, who discussed translocation into the brain and potential neurological damage following nanoparticle exposure;

* Corresponding author at: B105-05, Toxicity Assessment Division, U.S. Environmental Protection Agency, Research Triangle Park, NC 27711, USA. Tel.: +1 919 541 7538; fax: +1 919 541 4849.
E-mail addresses: boyes.william@epa.gov, Boyes.William@epamail.epa.gov (W.K. Boyes).

0161-813X/$ – see front matter. Published by Elsevier Inc.
doi:10.1016/j.neuro.2011.12.013

and Dr. William Boyes, who described the retina as a potential site of nanomaterial phototoxicity. Another symposium at the conference, to be reported elsewhere, focused on the exposure pathway involving inspired airborne particulate matter depositing into the nasal olfactory epithelium, being taken up and transported to the olfactory bulb and perhaps beyond to other brain regions. This potential route of exposure is discussed briefly in the current manuscript. Together the presentations at the conference and summarized here synthesize much of the current information regarding the potential uptake and distribution of nanomaterials to the nervous system and potential pathways through which ENMs might cause neurotoxic outcomes.

2. The toxicokinetics of engineered nanomaterials [R.A.Y.]

This presentation addressed how the mammalian organism handles metal/metal oxide ENMs, i.e., the toxicokinetics of ENMs, using nano-ceria as an example. This topic was reviewed in the classical context of the fate of materials: their absorption and bioavailability, distribution and translocation from the uptake to distal sites, metabolism (biotransformation), and elimination. It has been noted that more information on the absorption, distribution, metabolism and elimination (ADME) of nanoparticles is needed (Hagens et al., 2007), which may contribute to understanding their target sites and mechanisms of toxicity. ENM sizes are on the same scale as the molecular machinery of life, and might be handled by and affect the body similarly to like-sized molecules (Yokel and MacPhail, 2011).

2.1. Insoluble particles

Depending on the specific ENM and how researchers determine its presence, it may be unclear whether the intact ENM or dissolved components are measured. For example, elemental analysis (by ICP-MS, atomic absorption, etc.) of bulk tissue samples does not differentiate the intact ENM from dissolved components. Many metal/metal oxide ENMs can dissolve, releasing free ions (Brunner et al., 2006). Nanosilver readily dissolves, leading to uncertainty whether effects are from intact ENMs or released ions (Johnston et al., 2010). Zinc oxide ENMs are unstable in aqueous dispersion, undergoing Ostwald ripening and dissolution, e.g., releasing free zinc in Milli-Q water, cell culture media, yeast and zebrafish growth media, and endosomes (Bai et al., 2010; Heinlaan et al., 2008; Kasemets et al., 2009; Xia et al., 2008). Nano-copper (nano-Cu) dissolution readily occurs, e.g., releasing free copper in Milli-Q water, yeast growth medium, and in the stomach (Heinlaan et al., 2008; Kasemets et al., 2009; Meng et al., 2007). Although less soluble than zinc oxide ENM, iron oxide ENM is soluble in water; 81% dissolution was seen in monocytes in 24 h (Brunner et al., 2006; Zhu et al., 2009). Cadmium-containing quantum dots can disintegrate, due to surface oxidation, resulting in disintegration of quantum dot 705 (CdTe core, ZnS shell, methoxy-PEG5000 coating) in the kidney within 1 week (Derfus et al., 2004; Lin et al., 2009). However, some metal/metal oxide ENMs are poorly soluble (e.g., resistant to oxidation in vivo). Nano-ceria (cerium oxide, CeO_2), nano-titania (titanium dioxide, TiO_2) and nano-zirconia (zirconium oxide, ZrO_2) are insoluble in water (Brunner et al., 2006). Nano-titania is poorly soluble through the pH range of 3–11 (Schmidt and Vogelsberger, 2009). For example, nano-ceria was found to be insoluble in pH 4.5 artificial phagolysosomal fluid and OECD algae medium (He et al., 2010; Van Hoecke et al., 2009). Gold nanoparticles are also considered insoluble, as demonstrated by NIST's citrate-stabilized 10, 30, and 60 nm gold in aqueous dispersion (reference materials 8011, 8012 and 8013). The benefit of using a non-biodegradable ENM to study toxicokinetics is that elemental analysis indicates only the intact ENM rather than dissolved materials released from the particles. Insoluble ENM candidates for toxicokinetic studies include ceria as a metal oxide ENM because it has extensive commercial use; its very low endogenous and environmental levels make it easy to see the effects of exposure; analytical assays (e.g., ICP-MS) are very sensitive, enabling quantification (Yokel et al., 2009); and it is electron dense, enabling in vivo qualitative analysis and localization by electron microscopy (Hardas et al., 2010; Yokel et al., 2009). We have used polyhedral/cubic in-house synthesized and characterized 5–55 nm (mean width) ceria as a model metal oxide to study ENM distribution, persistence, and effects (Dan et al., 2012; Hardas et al., 2010; Yokel et al., submitted for publication). It has current commercial relevance as a diesel fuel additive to catalyze combustion and decrease combustion temperature and in chemico-mechanical planarization (integrated circuit manufacture). It is being investigated as a cardio- and neuroprotective therapeutic agent and is expected to have significant application in fuel cells and batteries. Similarly, gold is a good metal ENM candidate for toxicokinetic studies.

2.2. Absorption

The major exposure routes that pose concern for ENM absorption (uptake from its site of exposure into the systemic circulation) are inhalation and oral exposure. Due to the propensity of ENMs to agglomerate in air within minutes, airborne ENMs in occupational settings were most commonly described by a bimodal distribution; 200–400 and 2000–3000 nm in diameter (Brouwer, 2010; Seipenbusch et al., 2008). Some ENMs have been shown to be absorbed from the lung into the systemic circulation, followed by translocation/distribution to other organs and tissues. The distribution profile of carbon-, metal- and metal oxide-based ENMs after translocation from the lung is similar to that seen after their i.v. administration. They predominantly accumulate as agglomerates in the liver and spleen. For example, ceria concentration (mass/gram wet tissue) was highest in liver, and >spleen > kidney > heart, testis, and brain after intratracheal ceria ENM instillation. Approximately 0.1–1% of 7 nm ceria nanoparticles introduced by intratracheal instillation were absorbed from the lung and translocated to these organs after 1 month. This is based on a comparison of the percentage of the ceria ENM dose in these organs after intratracheal instillation to i.v. administration (He et al., 2010; Yokel et al., submitted for publication). Absorption from the nasal cavity directly into the brain via the olfactory nerve, into the olfactory bulb, and beyond (hippocampus, cerebral cortex and cerebellum), has been described for the polio virus (30 nm) (Bodian and Howe, 1941), colloidal silver-coated gold (50 nm) (de Lorenzo, 1970), ^{13}C particles (~35 nm) (Oberdörster et al., 2004), Mn (30 nm) (Elder et al., 2006), and iron oxide (280 nm) (Wang et al., 2007a). Similarly, there is the possibility of uptake into the maxillary division of the trigeminal nerve.

The extent of oral (gastrointestinal) ENM absorption is inversely related to ENM size, i.e., smaller particles have greater absorption (Hillyer and Albrecht, 2001; Jani et al., 1990). Using ceria as a model metal oxide ENM, from 0.00001% (for spleen, lung, heart, testis, and brain) to 0.01% (for liver) of the ceria given intragastrically was absorbed and then translocated to and retained in the liver, spleen, lung, kidney, heart, testis, and brain after 1 week. This conclusion was based on the comparison of the percentage of the ceria ENM dose in these organs after intragastric compared to i.v. administration (He et al., 2010; Yokel et al., submitted for publication).

In contrast to uptake from inhalation and oral exposure, intact skin greatly restricts, and in most cases prevents, ENM uptake. ENMs applied dermally, in the absence of organic solvents, do not appear to penetrate the intact skin as far as the stratum

granulosum or stratum spinosum (Yokel and MacPhail, 2011), from which ENMs could enter lymphatic or blood circulation. Quantum dots have shown deeper penetration into flexed healthy skin, but were still restricted to the top layers of the stratum corneum (Zhang and Monteiro-Riviere, 2008). However, 4 nm nano-TiO_2 repeatedly exposed to pig ear skin penetrated deep into the basal cell layer of the epidermis (Wu et al., 2009). After 60 days of dermal nano-TiO_2 (10–60 nm) exposure to hairless mice, Ti concentrations increased in the internal organs, suggesting systemic absorption (Wu et al., 2009).

2.3. Distribution

Little information on ENM distribution within blood has been reported. Twenty-five nm gold and 22, 25, and 80 nm titania entered erythrocytes, a non-phagocytic cell, suggesting distribution across the cell membrane (Geiser et al., 2005; Rothen-Rutishauser et al., 2006; Wang et al., 2007b). The distribution of 5, 15, 30, and 55 nm ceria in blood was studied in rats by repeated blood sampling after i.v. infusion of comparable doses (mass per body weight). Ten min after completion of the ceria ENM infusion, <2% of the 15, 30, and 55 nm ceria remained in circulating blood, compared to ~30% of the 5 nm ceria. The 5 nm ceria may not have been recognized by the reticuloendothelial system (a.k.a.: mononuclear phagocyte system) as readily as the larger ceria ENMs and was too large to be removed by glomerular filtration. Blood withdrawn 10, 30, 45, 60, 120, and 240 min after completion of i.v. infusions of 5–55 nm ceria was assayed by ICP-MS to determine total cerium content. Rather than a consistent decrease over time, as expected following i.v. administration, blood cerium concentration increased 4 h above all prior samples after administration of the 15 nm ceria ENM and was higher 0.5, 2 and 4 h after the 30 nm ceria ENM than the prior sample at each of these times. This might be explained by rapid distribution of the ceria to a site from which it was later released back into the blood. The distribution of ceria in blood serum compared to whole blood decreased over 4 h for the 15 and 30, but not 5 or 55, nm ceria ENM, suggesting a change in the surface properties of these ENMs. The migration of the 15 and 30 nm ceria into the clot fraction over time may be due to coating by protein or lipid adsorption to create a corona around the ENM (opsonization), resulting in greater association with blood cells (Dan et al., 2012).

2.4. Metabolism (biotransformation)

Aside from dissolution, opsonization is the most important biotransformation process. It is thought that the ENM surface coating is extremely important because it is what contacts cells and what cells "see" (Monopoli et al., 2011; Walczyk et al., 2010). Opsonization is believed to occur within seconds (Cherukuri et al., 2006; Owens and Peppas, 2006). Among the >2000 proteins in blood, many have been shown to opsonize ENMs. ENM composition and shape influence which proteins coat the nanomaterial (Deng et al., 2009; Monopoli et al., 2011).

2.5. Excretion

Renal glomerular filtration occurs for globular proteins and ENMs with a hydrodynamic diameter ≤~6 nm. For example, ~40 and 80%, respectively, of 5.5 and 4.4 nm quantum dots was excreted in urine in 4 h after i.v. injection (Choi et al., 2007), and 8.6% of a 1.4 nm gold ENM was excreted in urine and 5% in feces in 24 h (Semmler-Behnke et al., 2008). In contrast, less than 0.5% of a 30 nm ceria ENM was eliminated in urine and feces in two weeks, ~98% of which was via feces (Yokel et al., submitted for publication). This raises the question: If ceria ENM is not biodegraded or eliminated, what is its fate after entering systemic circulation? To address this, rats were infused with 30 nm ceria and terminated 1, 7, 30, or 90 days later; tissues were obtained from 17 organs/sites, blood, and cerebrospinal fluid, and their cerium content was determined. No statistically significant decrease of cerium was seen from the 1st to the 90th day in any organ. The presence of ceria ENM was verified by electron microscopy. Highest concentrations were seen in macrophages in reticuloendothelial tissues, as has been observed for other insoluble ENMs (Yokel et al., submitted for publication). These results illustrate prolonged retention of a non-degradable ENM, consistent with reports of titania (Fabian et al., 2008; van Ravenzwaay et al., 2009), gold (Cho et al., 2009b) and functionalized quantum dots (Ballou et al., 2004; Fischer et al., 2006; Lin et al., 2008; Yang et al., 2007). Within cells in reticuloendothelial tissues, the ceria ENM were often found in agglomerations (collections of particles loosely bound by relatively weak forces, such as van der Waals, electrostatic, surface tension, and physical entanglement). The prolonged persistence of these ceria agglomerates was associated with histopathological changes, including granulomatous formations in the spleen and liver.

2.6. Distribution to the brain

In contrast to ceria ENM accumulation in reticuloendothelial system tissues, the concentration of ceria in the brain was orders of magnitude lower (Yokel et al., submitted for publication). However, cerium determination in bulk brain samples that contain brain parenchyma and brain vasculature does not reveal whether the ceria was able to cross the blood–brain barrier (BBB), or if its distribution was limited to the vascular compartment and the cells that comprise the barriers between blood and brain. A review of literature reporting brain concentrations of insoluble metal and metal oxide ENMs (30 nm ceria, 1.4–100 nm gold, 50 and 100 nm silica, 25 nm titania and 13 nm quantum dots with determination of whether the ENM crossed the BBB, usually determined by electron microscopy, into brain parenchyma revealed most nanomaterials were either not seen in the brain or poorly entered the brain (Cho et al., 2009a; De Jong et al., 2008; Hardas et al., 2010; Semmler-Behnke et al., 2008; Sonavane et al., 2008; van Ravenzwaay et al., 2009; Yang et al., 2007; Yokel et al., 2009, unpublished). When expressed as a percentage of the dose that was seen in the brain, no reports were found of >0.5%. When compared to brain weight as a % of body weight (~0.5% for the rat and 1.75% for the mouse), no ENM concentrated in the brain. When the ENM in the blood within the vasculature of the brain was considered, very few reports showed more metal/metal oxide ENM in the brain than could be accounted for by the ENM in the blood in the blood vessels within the brain. The ENMs could have been adsorbed to the luminal wall of brain microvascular endothelial cells, been within those cells or the pericytes or astrocyte foot processes, or been retained by the basement membrane, and therefore not within brain parenchyma. The very low distribution of ENMs into the brain should not be surprising, given the well known restrictive properties of the BBB. Brain entry can be achieved by diffusion of lipophilic material ~<400 Da; uptake by phagocytic processes (caveolar- and clathrin-mediated endocytosis for ~60 and ~120 nm particles, respectively); and transporter-mediated endocytosis, e.g., for apolipoprotein-coated and transferrin-conjugated particles. The studies that found no or little brain ENM entry were conducted in mature rodents. ENM translocation to the brain has been seen in studies following *in utero* exposure. Agglomerates of 100–200 nm titania were seen by transmission electron microscopy (TEM) in brain 6 weeks postpartum after subcutaneous injection of 25–70 nm titania ENM into mice 3, 7, 10, and 14 days post coitum. Apoptosis in the brain indicated this fetal

titania exposure had adverse effects on development (Takeda et al., 2009). As expected, ENM distribution into the fetal brain was size dependent. Seventy, but not 300 or 1000 nm, silica ENM was seen in fetal brain as single particles after i.v. injection to pregnant mice (Yamashita et al., 2011).

2.7. Conclusions

Based on available results, some generalities can be stated about the toxicokinetics of metal/metal oxide ENMs. These particles are rapidly cleared from circulation. If they are not small enough to be filtered by renal glomeruli, they are primarily cleared from blood into reticuloendothelial tissues, where they are retained for a long time. A few reports have shown increases in the blood ENM concentration a few h after i.v. administration, suggesting short-term residence in a site outside of blood followed by re-entry into blood. This may be due to opsonization, changing of surface properties, and/or release from reticuloendothelial or lymphatic sites. The intact blood–brain barrier greatly limits or prevents metal/metal oxide ENMs from entering brain parenchyma. In summary, metal/metal oxide ENMs exhibit considerable toxicokinetic differences from other small molecules.

3. Translocation into the brain and potential damage following nanoparticle exposure [R.C. and C.C.]

3.1. Nose-to-brain transport

With increasing production and application, the toxicological effects of nanomaterials are currently of concern as a potential threat to human health. The BBB separates the brain interstitial fluid from the circulating blood and provides an efficient protective barrier to the CNS. It has been demonstrated that the nose-to-brain transport of exogenous materials is a potential route for bypassing the BBB (Brenneman et al., 2000; Illum, 2000; Oberdörster et al., 2009). For instance, ^{13}C nanoparticles can be transported directly from the olfactory epithelium to the olfactory bulb via the olfactory nerves (Oberdörster et al., 2004). Other nanoparticles including gold (de Lorenzo, 1970), manganese oxide (Elder et al., 2006), and ferric oxide (Wang et al., 2007a) have also been reported to accumulate in the olfactory bulb or even to penetrate deeply into the brain and induce damage. The olfactory bulb, as the first target site, will receive the earliest and highest dose following nasal exposure. It is proposed that a unique relationship between the anatomy and physiology of the mammalian nasal and cranial cavity tissues leads to the direct delivery of nanoparticles into the brain (Oberdörster et al., 2005).

3.2. Nano-copper

Nano-sized copper particles (nano-Cu) are used in agriculture and industries involving bactericides, air and liquid filtration, metallic coating on integrated circuits, batteries, sensors, catalysts, lubricant oils, brake linings, polymers and plastics. The many applications of Cu nanoparticles greatly increase the risk of their release into the environment. In our laboratory, the acute toxic effects of nano-Cu particles in mice have been evaluated. Based on animal experiments, oral LD_{50} values determined for 23.5 nm Cu particles, 17 μm Cu particles, and cupric ions were 413, >5000, and 110 mg/kg body weight, respectively (Chen et al., 2006). Our previous results showed pathological changes and severe injury in kidneys and liver of mice exposed to 23.5 nm Cu particles by a single oral gavage at a dose level of 1000 mg/kg body weight. However, these phenomena did not appear in the mice exposed to 17 μm Cu particles at the same exposure level and condition (Chen et al., 2006; Liu et al., 2009). After nasal instillation of Cu nanoparticles every two days for 15 days at a dosage of 10 or 40 mg/kg body weight, these particles accumulated mainly in the liver and lung and were associated with significant pathological changes. Compared to oral administration, nasal instillation led to significant particle accumulation and severe lesions to the olfactory bulb (Fig. 1A). The number of olfactory cells decreased and the external plexiform and mitral cell layers were disrupted. The laminated structure of the olfactory bulb was damaged, especially in the internal plexiform layer and granule cell layers. However, there were no obvious histopathological changes of brain tissues including the cerebellum (Liu et al., 2009; Zhang et al., in press). Therefore, the liver, lung, and olfactory bulb were not only the main accumulative tissues, but also sensitive organs where adverse effects of intranasally instilled nano-Cu particles occurred.

Monoamine neurotransmitters usually modulate various physiological processes of the body and have been used as sensitive markers for toxicity to the CNS (Chen et al., 2010; Li et al., 2009). Our recent results showed that intranasally instilled nano-Cu not only caused pathological lesions but also influenced neurotrans-

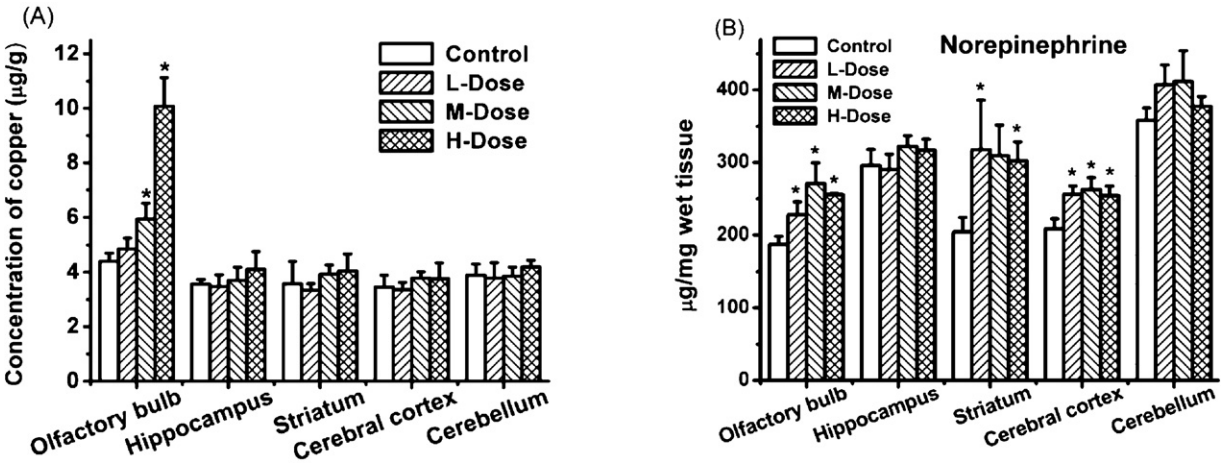

Fig. 1. Copper concentration (A) and associated norepinephrine levels (B) after intranasal instillation of copper nanoparticles. Mice were instilled with low, middle or high (1, 10, 40 mg/kg) doses of copper nanoparticles every two days for a total of 15 days ($n = 6$). Different brain regions were measured for copper concentration by ICP-MS, or measured for norepinephrine concentration by high performance liquid chromatography coupled with electrochemical detection. Data are shown as mean ± SD. An asterisk indicates a significant difference ($p < 0.05$) from the control group.
Data are modified from Zhang et al. (in press).

mitter levels in brain tissues. In our experiment, the levels of dopamine (DA) and homovanillic acid (HVA) were decreased, and 5-hydroxytryptamine (5-HT) and 5-hydroxyindoleacetic acid (5-HIAA) were increased in the olfactory bulb following nano-Cu instillation. Compared to controls, the levels of these monoamine neurotransmitters also changed in other CNS tissues such as the hippocampus, striatum, cerebral cortex, and cerebellum. The altered concentration of norepinephrine (Fig. 1B) showed that the normal function of the whole brain was disturbed after intranasal instillation of nano-Cu (Zhang et al., in press). It is clear that substantial respiratory exposure to Cu nanoparticles not only poses a risk to the olfactory bulb, but also influences neurotransmitter levels in CNS regions where nano-Cu particle accumulation was not observed.

3.3. Nano-TiO_2

Nanocrystalline TiO_2, a non-combustible and odorless powder, is an important material widely used in paints, waste water treatment, cosmetics, food additives, sterilization, biomedical ceramics, and implanted biomaterials. Our previous results showed that nasally instilled TiO_2 nanoparticles translocated into the murine brain, caused pathological lesions to the hippocampus and changed neurochemical levels in the brain (Wang et al., 2008b). We also found subtle neurotoxicity differences between responses to anatase and rutile TiO_2 crystal structures (Wang et al., 2008a). In recent work, we used various types of rutile TiO_2 particles with different sizes and surface modifications (i.e., uncoated micro- or nano-sized particles, which are hydrophobic), and surface coated nano-sized particles (which are hydrophilic and water-soluble) to evaluate neurotoxicity in mice following nasal instillation of 500 μg/mouse every two days for a total of 30 days. Micrometer-sized particles did not induce any lesion to neurons of the cerebral cortex or hippocampus, where Ti concentrations were not different from controls. Nanometer-sized TiO_2 particles, especially water-soluble particles, did induce obvious damage to the neurons of the cerebral cortex. Normal neuron density was decreased in the cerebral cortex by nanometer-sized particles. Neuron density was also decreased in the CA1 layer of the hippocampus, but only following intranasal instillation of water-soluble modified TiO_2 nanoparticles. The micrometer-sized TiO_2 particles did not influence the neuron density in cerebral cortex or hippocampus, possibly because the translocation of nanoparticles in the brain is partially dependent on particle size. Our ICP-MS results show that intranasally instilled hydrophilic TiO_2 nanoparticles translocated into the cerebral cortex and striatum of the murine brain, while hydrophobic TiO_2 nanoparticles of comparable size only accumulated in the striatum. This demonstrates that the surface modification of TiO_2 nanoparticles has an important influence on their translocation.

Compared to the micrometer-sized particles, only nanometer-sized particles showed accumulation and influenced the concentration levels of neurotransmitters in the brain. After intranasal instillation of TiO_2 particles for 30 days, hydrophobic micrometer-sized particles did not induce any changes in monoamine levels or any pathological lesions to the brain. Hydrophobic nanometer-sized particles influenced the 5-HT and 5-HIAA levels in the hippocampus and cerebellum, DA level in the cerebral cortex and cerebellum, as well as DOPAC in the cerebral cortex and striatum. Hydrophilic nanoparticles influenced the monoamine levels in all the studied sub-brain regions when compared with the group of hydrophobic nanoparticles, which further indicates that surface modification plays an important role in nanoparticle toxicity (Zhang et al., 2011). These studies show that the physicochemical properties of nanomaterials such as size and surface modification will influence their mammalian neurotoxicity.

3.4. Conclusions

Our results show that intranasally-instilled nanometer-sized Cu and TiO_2 particles can accumulate in the CNS through nose-to-brain transport. These nanoparticles within the CNS not only provoke pathological lesions to the brain but also influence monoamine levels in various sub-brain regions. Moreover, the size, surface chemistry and shape of the nanomaterials play important roles in their transportation and toxicity effects in the CNS. Altogether, serious consideration should be given to the physicochemical characters of nanomaterials when evaluating their neurological effects.

4. The retina as a potential site of nanomaterial phototoxicity [W.K.B.]

The retina is the only part of the central nervous system directly exposed to light. As such, materials that are prone to induce phototoxicity have a chance to be photo-neurotoxic in the retina and surrounding tissues. Light penetration to different ocular tissues is dependent on its wavelength (Roberts, 2002). The cornea filters wavelengths below approximately 290 nm, including UVC (100–280 nm) and a portion of the UVB spectrum (280–315 nm). Wavelengths of light between 295 and 400 nm can pass through the cornea but are absorbed by the lens of adult humans. These include wavelengths classified as UVA (315–400 nm). The full filtering capacity of the human lens develops slowly, however, and the eye of a juvenile human allows a portion of the UVA spectrum to penetrate the cornea and lens. According to Lerman (1983), the lens of a 3 day-old infant transmits about 80% of UVA radiation, and the portion of the UVA transmitted through the lens decreases slowly over years so that a 17 year old lens still transmits between 20 and 40% of UVA. Adult filtering levels were observed in the lens of a 25 year old. Non-primate mammals also transmit UVA to the retina. For example, whereas short wavelength sensitive cones of humans are responsive to blue light wavelengths, the analogous short-wavelength sensitive cones of rats are primarily sensitive to UVA (Jacobs et al., 2001). The potential distribution of phototoxic damage in the eye is therefore dependent on the wavelengths of light reaching the ocular tissues, which varies based on the species and age of the exposed subject.

4.1. Photoactive nanomaterials

Several ENMs are purposefully designed to be photoactive, with TiO_2 being a prime example (Fujishima et al., 2000; Kwon et al., 2008). The absorption of a photon of light elevates a surface electron of TiO_2 to the conduction band, leaving behind a valence band hole that extracts electrons from nearby molecules, including hydroxyl ions or water. This light-induced catalytic reaction sequence has potential utility for numerous commercial and environmental applications. The incorporation of TiO_2 into surface coatings such as paints or other building materials can lead to self-cleaning surfaces that could be applied to exterior or interior surfaces (Kwon et al., 2008). Photocatalytic degradation of hydrocarbons, pesticides, and other environmental pollutants is being considered for remediation of polluted water bodies or hazardous waste sites (Muneer et al., 2002; Yeo and Kang, 2006). TiO_2 photocatalysis may also be useful for sterilization of pathogen-contaminated water systems (Amezaga-Madrid et al., 2002). Fullerene and substituted fullerene derivatives are also photoactive, and these substances are being considered for applications such as photovoltaic devices.

Photoactivity and photocatalytic reactions can lead to phototoxicity. The hydroxyl radicals formed can reduce O_2, generating superoxide radicals, which in turn initiate a cascade of reactive

oxygen species (ROS) reactions. If the photoactivation of TiO_2 and the consequent ROS generation occurs in biological tissues, then oxidative damage may occur to lipids, proteins, nucleic acids, or other critical biological materials. The toxic consequences resulting from ROS production are common to many toxicity pathways.

4.2. TiO_2 phototoxicity

We have evaluated the phototoxic potential of nanomaterials including nano-TiO_2 in tissue culture using a human-derived immortalized cell line of retinal pigment epithelial cells (ARPE-19) (Sanders et al., 2011). The cells were grown in standard cell culture media in the presence of fetal bovine serum (FBS). Phenol red was omitted from the media because it is a potentially phototoxic substance. Nano-TiO_2 samples were dispersed in cell culture medium with FBS (concentration range 0.1–100 μg/ml). Dispersions without FBS aggregated rapidly and were unstable over time. The presence of serum stabilized the dispersion of the TiO_2 nanoparticles, likely through opsonization.

It was important to determine if the nanoparticles were taken up by the cells in vitro. We examined ARPE-19 cells treated with nano-TiO_2 using phase contrast and dark-field microscopy. Under dark-field imaging, the TiO_2 particles reflected large amounts of light due to their high refractive index and therefore appeared as bright star-like images against a dark background (Zucker et al., 2010). The superposition of dark-field and stained fluorescent images showed accumulations of TiO_2 particles surrounding the nuclei of ARPE-19 cells. Few nanoparticles were observed in the regions between cells on the tissue culture plates while numerous particles were observed inside the cells. The amount of material incorporated into each cell was dose-related. At low doses (0.1–3 μg/ml), only a few particles were observed inside cells. At high doses (30 μg/ml), the ARPE-19 cells amassed large quantities of what appeared to be agglomerated TiO_2 particles that in some cases were equivalent to the size of the cell nucleus (Zucker et al., 2010).

Flow cytometry confirmed that the TiO_2 nanoparticles were inside the ARPE-19 cells. Due to the high reflective properties of TiO_2 particles, there was a dose-related increase of the side scatter signal for cells treated with nano-TiO_2 (Sanders et al., 2011; Zucker et al., 2010).

To evaluate potential phototoxicity, ARPE-19 cells were plated into 24-well plates and treated with a dose range of TiO_2 (Sanders et al., 2011). The cells were allowed to incubate with the TiO_2 until the following day, when the culture plates were either kept in the dark or exposed to visible light or UVA radiation. The day after light or radiation treatment, a live/dead assay was conducted to evaluate viability of the treated cells relative to controls. The live/dead assay involved staining the cultures with calcein-AM, which stains cells with intact cell membranes and active metabolic machinery and are therefore assumed to be alive. Cultures were also co-stained with propidium iodide, which stains cells with disrupted cell membranes and are therefore assumed to be dead. The live and dead cells were counted from photographs of appropriately filtered microscope images to determine percent viability.

Six TiO_2 samples were evaluated that had a range of mean particle sizes (nominal range 10–250 nm; measured range 25–214 nm) and a mixture of anatase and rutile crystal structures (Table 1) (Sanders et al., 2011). The cells treated with TiO_2 and kept in the dark or exposed to visible light showed relatively low toxicity, depending on the sample. The most toxic sample in the dark was Degussa P25 (measured size 31 nm, anatase/rutile structure) which showed decreased viability at and above concentrations of 10 μg/ml (Fig. 2). Exposure to visible wavelengths of light (434–650 nm, 17.9 J/cm^2) did not alter the cytotoxicity of TiO_2 particles from that measured in the dark (data not shown). The toxicity of every TiO_2 sample was substantially increased by UVA treatment (330–383 nm, 7.5 J/cm^2), as shown in Table 1. The exposure to UVA alone did not reduce cell viability in the absence of TiO_2. The lower LC_{50} values for TiO_2 samples with UVA radiation were indicative of phototoxic reactions.

The presumed mechanism of phototoxicity involves the generation of ROS after activation of the photocatalytic TiO_2. This was evaluated using flow cytometry and the fluorescent marker Mitosox, which is sensitive to the production of ROS. As shown in Fig. 2, Mitosox fluorescence was increased in the dark, by TiO_2 at a

Table 1
TiO_2 nanoparticle samples evaluated for phototxicity.

Vendor	Analyzed[a] Crystal structure	Analyzed[b] TEM Avg size and (size range) (nm)	Analyzed Surface area BET (m^2/g)	LC_{50} (μg/ml)[c] in Dark	LC_{50} (μg/ml) after UVA
Alfa Aesar Stock # 39953 Lot # C27R043	94% anatase/ 6% rutile	22 (9–61)	49.8	>100 μg/ml	41.2
Alfa Aesar Stock # 44690 Lot # D22T034	Anatase	25 (6–60)	118	>100 μg/ml	4.9
Degussa Aeroxide P25 Lot # 4165012298	86% anatase/ 14% rutile	31 (12–88)	52.9	~100 μg/ml	4.5
Nanostructured and Amorphous Materials Inc. Stock # 5485HT Lot # 5485-030007	85% anatase/ 15% rutile	59 (36–97)	22.2	>100 μg/ml	47.1
Acros Organics Cat. # 21358 Lot # A0075656	Anatase	142 (67–322)	6.99	>100 μg/ml	62.8
Mknano MKN-TiO2-R250 Lot # 459/2007	Rutile	214 (37–410)	11.6	>100 μg/ml	77.4

Modified from Sanders et al. (2011).

[a] All samples >97% purity.
[b] TiO_2 physicochemical properties determined by an independent analysis performed by the University of Kentucky.
[c] The highest concentration tested was 100 μg/ml.

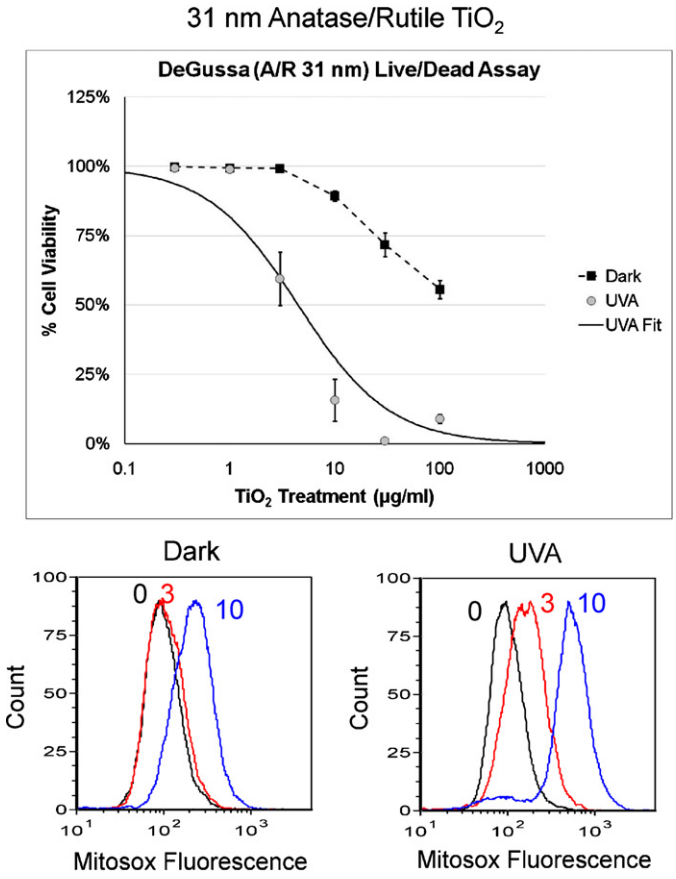

Fig. 2. The upper panel depicts the percentage of viable cells (mean ± SEM) determined in a live/dead assay of retinal pigment epithelial cells in vitro treated with different concentrations of 31 nm anatase/rutile TiO_2 for 24 h and then either kept in the dark or exposed to UVA irradiation. The lower two panels depict the amount of Mitosox fluorescence, indicative of ROS production, measured in a flow cytometer for cells treated with 0, 3 or 10 μg/ml TiO_2 and kept in the dark (left side) or exposed to UVA irradiation (right side). UVA irradiation increased the amount of Mitosox fluorescence and the cytotoxicity in cells treated with TiO_2. These results are indicative of a phototoxic reaction.
Data are modified from Sanders et al. (2011).

dose of 10 μg/ml; a concentration that also marked the beginning of cytotoxicity in the dark for this particle. Under UVA radiation, the Mitosox signal was increased at a lower TiO_2 dose (3 μg/ml) and to a greater extent at 10 μg/ml. These changes correspond to the greater cytotoxicity under UVA radiation, as seen in the upper portion of Fig. 2 (Sanders et al., 2011).

The relative phototoxicity of the six tested TiO_2 samples was evaluated as a function of several measured parameters, including measured primary particle size, surface area, and reactivity. The reactivity was determined in an acellular assay involving formation of thiobarbituric acid reactive substances (indicative of ROS generation) under darkness or UVA radiation. The LC_{50} values under UVA radiation of the six TiO_2 particle samples were directly correlated with particle size (smaller particles were more toxic), inversely correlated with surface area (larger surface areas were more toxic), and, with one exception, inversely correlated with reactivity (more reactive particles were more toxic). Overall, the results indicated that smaller TiO_2 particles, which had larger relative surface areas per unit mass, generated more ROS under UVA radiation and were more phototoxic than larger TiO_2 samples.

4.3. Fullerol phototoxicity

Separate experiments have shown that fullerol, a water-soluble hydroxylated fullerene, is phototoxic to both ARPE-19 and human-derived ocular lens epithelial cells. Whereas TiO_2 was phototoxic with only UVA radiation, fullerol was phototoxic under both UVA radiation and visible wavelengths of light (Roberts et al., 2008; Wielgus et al., 2010).

4.4. Conclusions

In summary, a number of nanomaterials are designed to be photocatalysts. If photocatalytic reactions lead to the generation of ROS in biological tissues, they are likely to cause phototoxic reactions. The retina is a unique neural tissue that is exposed to light throughout life and also is exposed to UVA radiation in young humans prior to maturation of the UVA-filtering capability of the lens. The human lens is also exposed to UVA radiation, which is a factor in age-related loss of transparency due to cataract formation. TiO_2 particles were phototoxic in vitro following UVA exposure. Fullerol was phototoxic following either UVA or visible light exposure. The parameters influencing phototoxicity of ENMs include the spectral sensitivity of the particle, particle size, surface area, and reactivity. The studies described here have limitations that are typically associated with in vitro toxicity studies. In particular, the extent to which these materials would reach the ocular tissues following direct contact or in vivo exposure is currently unknown. Direct contact of nanomaterials to the eye might result in absorption and penetration of the ocular tissues, however, the tear film contains both aqueous and lipid layers and the corneal epithelium has tight junctions that limit penetration. Developers of pharmaceutical products intended for intraocular activity are exploring nanomaterial encapsulation to enhance penetration following eye drop application (Nagpal et al., 2010; Seyfoddin et al., 2010), indicating that nanomaterials with selective solubility and size parameters can penetrate the eye after contact exposure. Nanomaterials that are systemically absorbed could be delivered to the eye via the circulatory system. The retina has a blood-retinal barrier that is similar to the BBB, and materials that cross the BBB might be expected to also enter the retina. Conversely, systemic materials excluded from the brain may likewise fail to reach the retina. Finally, the contribution of factors not represented in vitro such as repair mechanisms, antioxidants, lifestyle, health status, or other factors may all influence these considerations.

Overall, these studies demonstrated that the toxicity of photoactive nanomaterials can be increased by co-exposure to light or UVA radiation. It may be important to consider the potential for phototoxicity in the design and evaluation of future ENMs.

5. Overall summary

The development of new ENM technologies holds great promise for many and varied materials with numerous beneficial applications. The safe development of these materials, however, is dependent on the knowledge of properties that may cause unintended consequences, such as neurotoxicity. Among the primary concerns for neurotoxicity are the classical questions of ADME, in particular, do the materials enter the brain or other components of the nervous system? Answering this question is complicated by a number of factors including difficulties in distinguishing exogenous nanomaterials from elements that are normal constituents of tissue (e.g., Fe, Mn, Cu) and distinguishing effects due to particles from ionic and soluble molecules released from the particles (e.g., Ag). The study of ceria ENMs provides a good solution to these problems in that it is insoluble and not normally found in brain tissue. The study of ceria ENM revealed that very little systemically delivered ceria ENM entered the brain tissue proper. Similar results have been seen with other metal/metal oxide ENMs. Interestingly, very little systemically delivered

ceria was excreted and instead was retained in the body; a property reported for many insoluble metal/metal oxide- and carbon-based ENMs. Further work is warranted to understand the effects of ENM persistence in the organism. As opposed to the systemic route of delivery, it appears that several types of ENMs, including Cu and TiO_2, can be taken up by the nasal olfactory epithelium into the olfactory bulb and cause effects further into the brain. The potential mechanisms of action of ENMs are also of considerable importance. In this synopsis, attention was focused on a phototoxicity mechanism which may be unique to the retina among components of the CNS because the retina is the only part of the brain directly exposed to light. Retinal pigment epithelial cells, as well as ocular lens cells, were susceptible to phototoxic effects when co-exposed to UVA radiation or visible light and photoactive ENMs, such as TiO_2 or fullerol. The properties on ENMs that influenced uptake, distribution or toxicity included particle size, coating, surface modification, solubility and reactivity. The results discussed in this synopsis begin to provide an understanding of the properties that should be considered in the future development and application of ENMs.

Acknowledgments

Portions of this work were supported in part by US EPA STAR Grant No. RD-833772 and by the National Basic Research Program of China (Grant No. 2011CB933401) and Natural Science Foundation of China (Grant No. 10975040).

The TiO_2 phototoxicity studies described here were conducted primarily by Kristen Sanders, Laura Degn, William R. Mundy, Robert Zucker, and Kevin Dreher at the USEPA in Research Triangle Park, NC.

This manuscript has been reviewed by the National Health and Environmental Effects Research Laboratory, USEPA and approved for publication. Mention of trade names and commercial products does not constitute endorsement or recommendation for use.

References

Amezaga-Madrid P, Nevarez-Moorillon GV, Orrantia-Borunda E, Miki-Yoshida M. Photoinduced bactericidal activity against *Pseudomonas aeruginosa* by TiO_2 based thin films. FEMS Microbiol Lett 2002;211:183–8.

Bai W, Zhang Z, Tian W, He X, Ma Y, Zhao Y, et al. Toxicity of zinc oxide nanoparticles to zebrafish embryo: a physicochemical study of toxicity mechanism. J Nanopart Res 2010;12:1645–54.

Ballou B, Lagerholm BC, Ernst LA, Bruchez MP, Waggoner AS. Noninvasive imaging of quantum dots in mice. Bioconjug Chem 2004;15:79–86.

Bodian D, Howe HA. Experimental studies on intraneuronal spread of poliomyelitis virus. Bull Johns Hopkins Hosp 1941;69:248–67.

Brenneman KA, Wong BA, Buccellato MA, Costa ER, Gross EA, Dorman DC. Direct olfactory transport of inhaled manganese ((54)MnCl(2)) to the rat brain: toxicokinetic investigations in a unilateral nasal occlusion model. Toxicol Appl Pharmacol 2000;169:238–48.

Brouwer D. Exposure to manufactured nanoparticles in different workplaces. Toxicology 2010;269:120–7.

Brunner TJ, Wick P, Manser P, Spohn P, Grass RN, Limbach LK, et al. In vitro cytotoxicity of oxide nanoparticles: comparison to asbestos, silica, and the effect of particle solubility. Environ Sci Technol 2006;40:4374–81.

Chen Y-S, Hung Y-C, Lin L-W, Liau I, Hong M-Y, Huang GS. Size-dependent impairment of cognition in mice caused by the injection of gold nanoparticles. Nanotechnology 2010;21:485102.

Chen Z, Meng H, Xing G, Chen C, Zhao Y, Jia G, et al. Acute toxicological effects of copper nanoparticles in vivo. Toxicol Lett 2006;163:109–20.

Cherukuri P, Gannon CJ, Leeuw TK, Schmidt HK, Smalley RE, Curley SA, et al. Mammalian pharmacokinetics of carbon nanotubes using intrinsic near-infrared fluorescence. Proc Natl Acad Sci U S A 2006;103:18882–6.

Cho M, Cho WS, Choi M, Kim SJ, Han BS, Kim SH, et al. The impact of size on tissue distribution and elimination by single intravenous injection of silica nanoparticles. Toxicol Lett 2009a;189:177–83.

Cho WS, Cho M, Jeong J, Choi M, Cho HY, Han BS, et al. Acute toxicity and pharmacokinetics of 13 nm-sized PEG-coated gold nanoparticles. Toxicol Appl Pharmacol 2009b;236:16–24.

Choi HS, Liu W, Misra P, Tanaka E, Zimmer JP, Itty Ipe B, et al. Renal clearance of quantum dots. Nat Biotechnol 2007;25:1165–70.

Dan M, Wu P, Grulke EA, Graham UM, Unrine JM, Yokel RA. Ceria engineered nanomaterial distribution in and clearance from blood: size matters. Nanomedicine 2012;7:95–110.

De Jong WH, Hagens WI, Krystek P, Burger MC, Sips AJ, Geertsma RE. Particle size-dependent organ distribution of gold nanoparticles after intravenous administration. Biomaterials 2008;29:1912–9.

de Lorenzo AJD. The olfactory neuron and the blood–brain barrier. In: Wolstenholme G, Knight J, editors. Taste and smell in vertebrates. London: Churchill; 1970 , pp. 151–76.

Deng ZJ, Mortimer G, Schiller T, Musumeci A, Martin D, Minchin RF. Differential plasma protein binding to metal oxide nanoparticles. Nanotechnology 2009;20 455101/455101–455101/455109.

Derfus AM, Chan WCW, Bhatia SN. Probing the cytotoxicity of semiconductor quantum dots. Nano Lett 2004;4:11–8.

Elder A, Gelein R, Silva V, Feikert T, Opanashuk L, Carter J, et al. Translocation of inhaled ultrafine manganese oxide particles to the central nervous system. Environ Health Perspect 2006;114:1172–8.

Fabian E, Landsiedel R, Ma-Hock L, Wiench K, Wohlleben W, van Ravenzwaay B. Tissue distribution and toxicity of intravenously administered titanium dioxide nanoparticles in rats. Arch Toxicol 2008;82:151–7.

Fischer HC, Liu L, Pang KS, Chan WCW. Pharmacokinetics of nanoscale quantum dots: in vivo distribution, sequestration, and clearance in the rat. Adv Funct Mater 2006;16:1299–305.

Fujishima A, Rao TN, Tryk DA. Titanium dioxide photocatalysis. J Photochem Photobiol C Photochem Rev 2000;1:1–21.

Geiser M, Rothen-Rutishauser B, Kapp N, Schurch S, Kreyling W, Schulz H, et al. Ultrafine particles cross cellular membranes by nonphagocytic mechanisms in lungs and in cultured cells. Environ Health Perspect 2005;113:1555–60.

Hagens WI, Oomen AG, de Jong WH, Cassee FR, Sips AJ. What do we (need to) know about the kinetic properties of nanoparticles in the body. Regul Toxicol Pharmacol 2007;49:217–29.

Hardas SS, Butterfield DA, Sultana R, Tseng MT, Dan M, Florence RL, et al. Brain distribution and toxicological evaluation of a systemically delivered engineered nanoscale ceria. Toxicol Sci 2010;116:562–76.

He X, Zhang H, Ma Y, Bai W, Zhang Z, Lu K, et al. Lung deposition and extrapulmonary translocation of nano-ceria after intratracheal instillation. Nanotechnology 2010;21 285103/285101–285103/285108.

Heinlaan M, Ivask A, Blinova I, Dubourguier H-C, Kahru A. Toxicity of nanosized and bulk ZnO, CuO and TiO_2 to bacteria *Vibrio fischeri* and crustaceans *Daphnia magna* and *Thamnocephalus platyurus*. Chemosphere 2008;71:1308–16.

Hillyer JF, Albrecht RM. Gastrointestinal persorption and tissue distribution of differently sized colloidal gold nanoparticles. J Pharm Sci 2001;90:1927–36.

Illum L. Transport of drugs from the nasal cavity to the central nervous system. Eur J Pharm Sci 2000;11:1–18.

Jacobs GH, Fenwick JA, Williams GA. Cone-based vision of rats for ultraviolet and visible lights. J Exp Biol 2001;204:2439–46.

Jani P, Halbert GW, Langridge J, Florence AT. Nanoparticle uptake by the rat gastrointestinal mucosa: quantitation and particle size dependency. J Pharm Pharmacol 1990;42:821–6.

Johnston HJ, Hutchison G, Christensen FM, Peters S, Hankin S, Stone V. A review of the in vivo and in vitro toxicity of silver and gold particulates: particle attributes and biological mechanisms responsible for the observed toxicity. Crit Rev Toxicol 2010;40:328–46.

Kasemets K, Ivask A, Dubourguier HC, Kahru A. Toxicity of nanoparticles of ZnO, CuO and TiO_2 to yeast *Saccharomyces cerevisiae*. Toxicol In Vitro 2009;23:1116–22.

Kwon S, Fan M, Cooper AT, Yang H. Photocatalytic applications of micro- and nano-TiO_2 in environmental engineering. Crit Rev Environ Sci Technol 2008;38:197–226.

Lerman S. NMR fluorescence spectroscopy on the normal, aging, and cataractous lens. Lens Res 1983;1:175.

Li N, Guo J, Liu B, Yu Y, Cui H, Mao L, et al. Determination of monoamine neurotransmitters and their metabolites in a mouse brain microdialysate by coupling high-performance liquid chromatography with gold nanoparticle-initiated chemiluminescence. Anal Chim Acta 2009;645:48–55.

Lin CH, Chang LW, Chang H, Yang MH, Yang CS, Lai WH, et al. The chemical fate of the Cd/Se/Te-based quantum dot 705 in the biological system: toxicity implications. Nanotechnology 2009;20 215101/215101–215101/215109.

Lin P, Chen JW, Chang LW, Wu JP, Redding L, Chang H, et al. Computational and ultrastructural toxicology of a nanoparticle, Quantum Dot 705, in mice. Environ Sci Technol 2008;42:6264–70.

Liu Y, Gao Y, Zhang L, Wang T, Wang J, Jiao F, et al. Potential health impact on mice after nasal instillation of nano-sized copper particles and their translocation in mice. J Nanosci Nanotechnol 2009;9:6335–43.

Meng H, Chen Z, Xing G, Yuan H, Chen C, Zhao F, et al. Ultrahigh reactivity and grave nanotoxicity of copper nanoparticles. J Radioanal Nucl Chem 2007;272:595–8.

Monopoli MP, Walczyk D, Campbell A, Elia G, Lynch I, Bombelli FB, et al. Physical–chemical aspects of protein corona: relevance to in vitro and in vivo biological impacts of nanoparticles. J Am Chem Soc 2011;133:2525–34.

Muneer M, Singh HK, Bahnemann D. Semiconductor-mediated photocatalysed degradation of two selected priority organic pollutants, benzidine and 1,2-diphenylhydrazine, in aqueous suspension. Chemosphere 2002;49:193–203.

Nagpal K, Singh S, Mishra D. Chitosan nanoparticles: a promising system in novel drug delivery. Chem Pharm Bull 2010;58:1423–30.

National Science and Technology Council. The National Nanotechnology Initiative – Strategic Plan. Arlington, VA: National Science and Technology Council, Committee on Technology and Subcommittee on Nanoscale Science Engineering and Technology; 2007.

Oberdörster G, Elder A, Rinderknecht A. Nanoparticles and the brain: cause for concern. J Nanosci Nanotechnol 2009;9:4996–5007.
Oberdörster G, Maynard A, Donaldson K, Castranova V, Fitzpatrick J, Ausman K, et al. Principles for characterizing the potential human health effects from exposure to nanomaterials: elements of a screening strategy, A report from the ILSI Research Foundation/Risk Science Institute Nanomaterial Toxicity Screening Working Group. Part Fibre Toxicol 2005;2:1–35.
Oberdörster G, Sharp Z, Atudorei V, Elder A, Gelein R, Kreyling W, et al. Translocation of inhaled ultrafine particles to the brain. Inhal Toxicol 2004;16:437–45.
Owens DE, Peppas NA. Opsonization, biodistribution, and pharmacokinetics of polymeric nanoparticles. Int J Pharm 2006;307:93–102.
Roberts JE. Screening for ocular phototoxicity. Int J Toxicol 2002;21:491–500.
Roberts JE, Wielgus AR, Boyes WK, Andley U, Chignell CF. Phototoxicity and cytotoxicity of fullerol in human lens epithelial cells. Toxicol Appl Pharmacol 2008;228:49–58.
Rothen-Rutishauser BM, Schurch S, Haenni B, Kapp N, Gehr P. Interaction of fine particles and nanoparticles with red blood cells visualized with advanced microscopic techniques. Environ Sci Technol 2006;40:4353–9.
Sanders K, Degn LL, Mundy WR, Zucker R, Dreher K, Zhao B, et al. In vitro phototoxicity and hazard identification of nano-scale titanium dioxide. Toxicol Appl Pharmacol 2011. doi: 10.1016/j.taap.2011.10.023.
Schmidt J, Vogelsberger W. Aqueous long-term solubility of titania nanoparticles and titanium(IV) hydrolysis in a sodium chloride system studied by adsorptive stripping voltammetry. J Solution Chem 2009;38:1267–82.
Seipenbusch M, Binder A, Kasper G. Temporal evolution of nanoparticle aerosols in workplace exposure. Ann Occup Hyg 2008;52:707–16.
Semmler-Behnke M, Kreyling WG, Lipka J, Fertsch S, Wenk A, Takenaka S, et al. Biodistribution of 1.4- and 18-nm gold particles in rats. Small 2008;4:2108–11.
Seyfoddin A, Shaw J, Al-Kassas R. Solid lipid nanoparticles for ocular drug delivery. Drug Deliv 2010;17:467–89.
Sonavane G, Tomoda K, Makino K. Biodistribution of colloidal gold nanoparticles after intravenous administration: effect of particle size. Colloids Surf B Biointerfaces 2008;66:274–80.
Takeda K, Suzuki K-i, Ishihara A, Kubo-Irie M, Fujimoto R, Tabata M, et al. Nanoparticles transferred from pregnant mice to their offspring can damage the genital and cranial nerve systems. J Health Sci 2009;55:95–102.
Van Hoecke K, Quik JTK, Mankiewicz-Boczek J, De Schamphelaere KAC, Elsaesser A, Van der Meeren P, et al. Fate and effects of CeO_2 nanoparticles in aquatic ecotoxicity tests. Environ Sci Technol 2009;43:4537–46.
van Ravenzwaay B, Landsiedel R, Fabian E, Burkhardt S, Strauss V, Ma-Hock L. Comparing fate and effects of three particles of different surface properties: nano-TiO_2, pigmentary TiO_2 and quartz. Toxicol Lett 2009;186:152–9.
Walczyk D, Bombelli FB, Monopoli MP, Lynch I, Dawson KA. What the cell sees in bionanoscience. J Am Chem Soc 2010;132:5761–8.
Wang B, Feng W, Wang M, Shi J, Zhang F, Ouyang H, et al. Transport of intranasally instilled Fine Fe_2O_3 particles into the brain: micro-distribution, chemical states, and histopathological observation. Biol Trace Elem Res 2007a;118: 233–43.
Wang J, Chen C, Liu Y, Jiao F, Li W, Lao F, et al. Potential neurological lesion after nasal instillation of TiO_2 nanoparticles in the anatase and rutile crystal phases. Toxicol Lett 2008a;183:72–80.
Wang J, Liu Y, Jiao F, Lao F, Li W, Gu Y, et al. Time-dependent translocation and potential impairment on central nervous system by intranasally instilled TiO_2 nanoparticles. Toxicology 2008b;254:82–90.
Wang J, Zhou G, Chen C, Yu H, Wang T, Ma Y, et al. Acute toxicity and biodistribution of different sized titanium dioxide particles in mice after oral administration. Toxicol Lett 2007b;168:176–85.
Wielgus AR, Zhao B, Chignell CF, Hu D-N, Roberts JE. Phototoxicity and cytotoxicity of fullerol in human retinal pigment epithelial cells. Toxicol Appl Pharmacol 2010;242:79–90.
Wu J, Liu W, Xue C, Zhou S, Lan F, Bi L, et al. Toxicity and penetration of TiO_2 nanoparticles in hairless mice and porcine skin after subchronic dermal exposure. Toxicol Lett 2009;191:1–8.
Xia T, Kovochich M, Liong M, Madler L, Gilbert B, Shi H, et al. Comparison of the mechanism of toxicity of zinc oxide and cerium oxide nanoparticles based on dissolution and oxidative stress properties. ACS Nano 2008;2:2121–34.
Yamashita K, Yoshioka Y, Higashisaka K, Mimura K, Morishita Y, Nozaki M, et al. Silica and titanium dioxide nanoparticles cause pregnancy complications in mice. Nat Nanotechnol 2011;6:321–8.
Yang RS, Chang LW, Wu JP, Tsai MH, Wang HJ, Kuo YC, et al. Persistent tissue kinetics and redistribution of nanoparticles, quantum dot 705, in mice: ICP-MS quantitative assessment. Environ Health Perspect 2007;115:1339–43.
Yeo MK, Kang M. Photodecomposition of bisphenol A on nanometer-sized TiO_2 thin film and the associated biological toxicity to zebrafish (*Danio rerio*) during and after photocatalysis. Water Res 2006;40:1906–14.
Yokel RA, Au TC, MacPhail R, Hardas SS, Butterfield DA, Sultana R, et al. Distribution, elimination and biopersistence to 90 days of a systemically-introduced 30 nm ceria engineered nanomaterial in rats; submitted for publication.
Yokel RA, Florence RL, Unrine JM, Tseng MT, Graham UM, Wu P, et al. Biodistribution and oxidative stress effects of a systemically-introduced commercial ceria engineered nanomaterial. Nanotoxicology 2009;3:234–48.
Yokel RA, MacPhail RC. Engineered nanomaterials: exposures, hazards and risk prevention. J Occup Med Toxicol 2011;6:1–27.
Zhang L, Bai R, Li B, Ge C, Du J, Liu Y, et al. Rutile TiO_2 particles exert size and surface coating dependent retention and lesions on the murine brain. Toxicol Lett 2011;207:73–81.
Zhang L, Bai R, Liu Y, Meng L, Li B, Wang L, et al. The dose-dependent toxicological effects and potential perturbation on the neurotransmitter secretion in brain following intranasal instillation of copper nanoparticles. Nanotoxicology, doi:10.3109/17435390.2011.590906, in press.
Zhang LW, Monteiro-Riviere NA. Assessment of quantum dot penetration into intact, tape-stripped, abraded and flexed rat skin. Skin Pharmacol Physiol 2008;21:166–80.
Zhu MT, Feng WY, Wang Y, Wang B, Wang M, Ouyang H, et al. Particokinetics and extrapulmonary translocation of intratracheally instilled ferric oxide nanoparticles in rats and the potential health risk assessment. Toxicol Sci 2009;107: 342–51.
Zucker RM, Massaro EJ, Sanders KM, Degn LL, Boyes WK. Detection of TiO_2 nanoparticles in cells by flow cytometry. Cytometry A 2010;77A:677–85.